JOURNAL OF COMPUTATIONAL PHYSICS 7, 12–31 (1971)

On the Stability of Poiseuille Flow in a Pipe*

H. J. CROWDER† AND C. DALTON

Department of Mechanical Engineering
University of Houston, Houston, Texas 77004

Received February 19, 1970

The problem of the stability of Poiseuille pipe flow was studied numerically. The finite-difference equations which were solved are approximations to the nonlinear, axisymmetric, Navier–Stokes equations in cylindrical coordinates subject to a stream function perturbation. The disturbance to the stream function is of the form $A_m(R_1^2/2 - R_1^4/4)\sin(A_r t)$, which is axisymmetric, oscillatory, and fixed in space. The resulting solutions show the experimentally observed instability of the stream function and vorticity at Reynolds numbers of 10,000 and 100,000 for a finite-amplitude disturbance, $A_m = 1.0$. The experimentally observed stability at a Reynolds number of 1000 and $A_m = 1.0$ was also found. At a Reynolds number of 3000 and $A_m = 1.0$, a neutral stability effect was noted. For a small-amplitude case, $A_m = 0.1$, at a Reynolds number of 100,000, the solution represents a damped disturbance which is consistent with classical small-amplitude theory.

1. INTRODUCTION

The stability problem for Poiseuille pipe flow has been of interest for many years. Osborne Reynolds (1880) first studied the problem experimentally and found that the laminar flow became unstable when $R = Wd/\nu$ was nearly 13,000, where W is the average velocity over the pipe cross section, d is the pipe diameter, and ν is the kinematic viscosity of the fluid. Further experiments by different investigators [Leite (1959), Bhat (1966), Kuethe (1956)] have shown that the critical, or transition, Reynolds number varies from approximately 2,000 to more than 40,000; the more idealized the flow conditions, the greater the critical Reynolds number.

Analytical studies of instability in pipe flow began with Sexl (1927) who used a small-perturbation theory in his approach to the problem. Others (Corcos and Sellars (1959) and Gill (1965) are the most prominent) have also contributed to the axisymmetric approach begun by Sexl. However, the small-perturbation

* Supported by NASA Contract No. NGR 44-005-065.

† Present address: TRW Systems Group, San Bernardino, California.

theory approach has not yielded instability at any Reynolds number, regardless of how large the value might be.

The current general consensus is that Poiseuille pipe flow is computationally stable to infinitesimal disturbances at large Reynolds numbers. This conclusion is based on the failure of the small-disturbance approach to predict the onset of turbulence while the experimental evidence is that turbulence is produced provided that the disturbance and Reynolds number are sufficiently large

The experimental instability has been attributed to entrance effects, surface roughness, external vibrations, and to the instability of the growing boundary layer as the flow develops in the entrance region. However, experiments can be conducted with the first three possible causes eliminated to examine the boundary-layer instability idea. Tatsumi (1952) studied the boundary-layer instability concept with asixymmetric disturbances and found that the critical Reynolds number was nearly 10,000.

The asymptotic series approach taken by Corcos and Sellers (1959) and by Gill (1965) produced results inconsistent with experiment since the series approach yielded no instability of the flow. This opens the question of whether a strictly numerical approach would not be more appropriate in determining features of Poiseuille pipe flow when subjected to an axisymmetric disturbance. Davey and Drazin (1969) sought a numerical (finite-difference) solution to the instability problem in considering yet another attempt at the axisymmetric small-disturbance problem first formulated by Sexl (1927). Davey and Drazin obtained numerical results which were consistent with the asymptotic series results obtained by Corcos and Sellars, and Gill. Again, the axisymmetric small-disturbance approach yielded results which were not consistent with experiment when the experimental Reynolds number is sufficiently high. Graebel (1970) considered a small-amplitude azimuthal disturbance and found instability for azimuthal wavenumbers greater than two. However, the corresponding minimum Reynolds numbers were much too low to correspond to experimental values. In spite of this apparent shortcoming, Graebel's study appears very promising for it has apparently opened the way for further studies of the azimuthal disturbance component.

2. Analysis

A more accurate and meaningful numerical approach would be to consider the nonlinear problem in its full form and apply the appropriate boundary and initial conditions in order to represent an axisymmetric finite-amplitude disturbance. The nondimensional Navier–Stokes equations are the governing differential equations, along with the continuity equation

$$\frac{\partial \bar{V}}{\partial t} + \bar{V} \cdot \nabla \bar{V} + \nabla p - \frac{1}{R} \nabla^2 \bar{V} = 0 \tag{1}$$

and

$$\nabla \cdot \bar{V} = 0. \tag{2}$$

In Eqs. (1) and (2), $\bar{V}$ is the nondimensional velocity vector, p is the nondimensional pressure, t is the nondimensional time, R is the Reynolds number, and ∇ is the nondimensional gradient operator in cylindrical coordinates.

After elimination of the pressure from Eqs. (1) and (2), we define the vorticity, Ω, by

$$\Omega = u_z - w_r \tag{3}$$

and introduce the stream function, ψ, by

$$u = -\frac{\psi_z}{r} \tag{4}$$

and

$$w = \frac{\psi_r}{r}, \tag{5}$$

so that the governing equations now become

$$\Omega_t - \left(\frac{\psi_z}{r}\,\Omega\right)_r + \left(\frac{\psi_r}{r}\,\Omega\right)_z = \frac{1}{R}\left[\left(\frac{1}{r}\,(r\Omega)_r\right)_r + \Omega_{zz}\right] \tag{6}$$

and

$$\Omega = -\frac{1}{r}\left[\psi_{zz} + r\left(\frac{\psi_r}{r}\right)_r\right]. \tag{7}$$

Simultaneous solution of Eqs. (6) and (7) for Ω and ψ yield the description of the flow field for whatever physical problem is described by the imposed boundary conditions. This approach has been followed by Fromm and Harlow (1963, 1963, 1964) in a variety of problems, and by Thoman and Szewczyk (1969) and Hirota and Miyakoda (1955), both for developing flow around a circular cylinder. Greenspan *et al.* (1964), Payne (1958), Ingham (1968), Briley (1968), and Dennis and Shimshoni (1964) have also used this approach for various problems.

Of all the publications in this area, the most closely allied work is that by Dixon and Hellums (1967), who treated both the stability of Poiseuille flow and plane Poiseuille flow. Their results in the case of plane Poiseuille flow show the experimentally observed instability, but in the case of Poiseuille flow they have shown only that a disturbance imposed on the field uniformly on a radius is amplified at a Reynolds number of 100,000. At a Reynolds number of 10,000, the results of their calculation show that the disturbance may either be amplifying

or decaying. At a Reynolds number of 1000 this solution shows the experimentally observed decay of the disturbance. Their calculation procedure was to use the alternating direction–iteration (ADI) method for solution of the vorticity transport equation and successive over-relaxation for solution of the stream-function equation. They obtained stream-function values only at every odd time step. They also used downstream boundary conditions which introduce periodicity into the flow field. Still, on the whole, their results seem to be valid. Our calculation procedure, disturbance, and downstream boundary conditions differ considerably from those used by Dixon and Hellums.

For the application of Eqs. (6) and (7) to the problem of Poiseuille flow in a pipe subject to a finite-amplitude disturbance, it is convenient to break both ψ and Ω into two parts each. Therefore, let

$$\psi(r, z, t) = F(r) + f(r, z, t) \tag{8}$$

and

$$\Omega(r, z, t) = G(r) + g(r, z, t), \tag{9}$$

where F and G refer to the main flow and f and g refer to any perturbation of the main flow.

Since F and G are main flow quantities for Poiseuille pipe flow, they are given in dimensionless form by

$$F(r) = \tfrac{1}{2}r^2 - \tfrac{1}{4}r^4 \tag{10}$$

and

$$G(r) = 2r. \tag{11}$$

Therefore, Eqs. (6) and (7) can be written as

$$g_t - f_z\left(\frac{g}{r}\right) + \frac{f_r g_z}{r} + (1 - r^2)\, g_z = \frac{1}{R}\left[\left(\frac{1}{r}(rg)_r\right)_r + g_{zz}\right] \tag{12}$$

and

$$f_{zz} + r\left(\frac{f_r}{r}\right)_r = -rg. \tag{13}$$

It should be noted that, to this point in the development, no assumption has been made which linearizes Eqs. (12) and (13); therefore, the equations are suitable for describing the behavior of the flow for both large- and small-amplitude disturbances.

The region over which Eqs. (12) and (13) are to be solved is an axisymmetric dimensionless field. The length L in the axial direction z of the field is much

greater than unity. The line $r = 0$ represents the center line of the pipe and $r = 1$ represents the wall.

The boundary conditions applied at $r = 1$ are the normal conditions of no slip and no flow through a solid boundary,

$$u = -\frac{f_z}{r} = 0 \tag{14}$$

and

$$w = \frac{f_r}{r} = 0. \tag{15}$$

Axial symmetry at the center line, $r = 0$, implies that

$$f_r = u_r = g_r = w_r = 0. \tag{16}$$

Since the governing differential equations (12) and (13) are singular on the line $r = 0$, and we demand that every quantity be bounded on that line, we have

$$u = u_r = w_r = g = f_z = f_r = g_r = g_z = 0. \tag{17}$$

On the line $z = 0$, fully developed pipe flow must exist; therefore, we have

$$g = 0 \qquad \text{on} \quad z = 0. \tag{18}$$

In order to make the solution as free as possible on $z = 0$, we use the condition

$$f_z = 0, \tag{19}$$

which allows the streamlines to move radially.

The downstream boundary conditions are somewhat harder to specify. Ideally, they are specified such that L is located so that no further change occurs in the solution by increasing L. We have followed the suggestion of Thoman and Szewczyk (1969) of using

$$f_{zz} = 0, \tag{20}$$

and either

$$g_{zz} = 0 \tag{21a}$$

or

$$g_z = 0, \tag{21b}$$

since use of $f_{zz} = Af$ and $g_{zz} = Bg$ imply periodicity of the flow field for A and B not equal to zero. Boundary conditions (20) and either of (21) do not imply the undesired periodicity of the flow field. It should be noted that these conditions

are an approximation to the condition that derivatives along a streamline are zero either for $L \gg 1$, or for streamlines parallel to the z axis.

Two considerations govern the form of the disturbance function which may be chosen. First, the disturbance should be modeled on a physically realizable system. Second, the disturbance function should not violate the continuity equation. The function

$$f(R_1, Z_1, t \geqslant 0) = \left(\frac{R_1^2}{2} - \frac{R_1^4}{4}\right) A_m \sin A_r t, \tag{22}$$

provides a mathematical disturbance to the stream function which is quite similar to the form of a disturbance generated by an infinitesimally thin hollow cylinder which is oscillated axially about the point (R_1, Z_1), where A_m is the amplitude and A_r is the period of the disturbance with $0 < R_1 < 1$ and $0 < Z_1 \ll L$. This type of disturbance is similar to that used by Leite (1959). Application of Eq. (13) yields the vorticity at the point (R_1, Z_1) as

$$g(R_1, Z_1 t \geqslant 0) = \frac{1}{R_1}\left(f_{rr} - \frac{f_r}{R_1} + f_{zz}\right). \tag{23}$$

Since we assume that the disturbance is generating any deviation from the fully developed flow solution, we have for initial conditions

$$f(r, z, 0) = 0 \tag{24}$$

and

$$g(r, z, 0) = 0 \tag{25}$$

for

$$0 \leqslant r \leqslant 1, \qquad 0 \leqslant z \leqslant L.$$

Now we turn to the boundary condition for g on the line $r = 1$. Since $r = 1$ is a solid boundary and $f_z = 0$ at every point on $r = 1$, we also have $f_{zz} = 0$. Therefore, we substitute this condition with Eq. (15) into Eq. (13) to obtain

$$g = -\frac{f_{rr}}{r} \qquad \text{on} \quad r = 1. \tag{26}$$

For the boundary and initial conditions to be consistent, we must have

$$f(0, z, t) = 0 \tag{27a}$$

and

$$g(0, z, t) = 0. \tag{27b}$$

3. The Finite-Difference Equations

For the purpose of computation, the differential operators equation in (12) are replaced by difference operators in the following way:

$$g(r, z, t) \rightarrow g^n_{i,j} = g(r_i, z_j, t_n), \tag{28a}$$

$$g_r = \frac{1}{2\Delta r}[g^n_{i+1,j} - g^n_{i-1,j}] + O(\Delta r^2), \tag{28b}$$

$$g_z = \frac{1}{2\Delta z}[g^n_{i,j+1} - g^n_{i,j-1}] + O(\Delta z^2), \tag{28c}$$

$$g_t = \frac{1}{\Delta t}[g^{n+1}_{i,j} - g^n_{i,j}] + O(\Delta t), \tag{28d}$$

$$g_{rr} = \frac{1}{\Delta r^2}[g^n_{i+1,j} - 2g^n_{i,j} + g^n_{i-1,j}] + O(\Delta r^2), \tag{28e}$$

and

$$g_{zz} = \frac{1}{\Delta z^2}[g^n_{i,j+1} - 2g^n_{i,j} + g^n_{i,j-1}] + O(\Delta z^2), \tag{28f}$$

with like definitions for $f(r, z, t)$ and its derivatives. The grid system initially chosen was a nonsquare, nonuniform system, but numerical experimentation indicated that equal spacing in both coordinate directions yielded a more accurate solution. Experimentation with the grid spacing showed that mesh spacings of 0.1 in both the radial and axial directions was satisfactory. For a more detailed discussion of this and other points involving the grid system, see Appendix B, Crowder and Dalton (1969).

The differential equation governing the stream function, Eq. (13), can be written in the following forms:

$$\rho_k f - f_{zz} = \rho_k f + f_{rr} - \frac{1}{r} f_r + rg \tag{29}$$

and

$$\rho_k f - f_{rr} + \frac{1}{r} f_r = \rho_k f + f_{zz} + rg, \tag{30}$$

by adding the quantity $\rho_k f$ to both sides and factoring the equations appropriately. This technique is the ADI method of solving a difference equation. Substitution of the necessary derivatives from Eq. (28) into Eqs. (29) and (30) yields

$$\rho_k f^{n+1,k+1}_{i,j} - (f^{n+1}_{i,j})^{k+1}_{zz} = \rho_k f^{n+1,k}_{i,j} + (f^{n+1}_{i,j})^k_{rr} - \frac{1}{r_i}(f^{n+1}_{i,j})^k_r + r_i g^{n+1}_{i,j} \tag{31a}$$

and

$$\rho_k f_{i,j}^{n+1,k+2} - (f_{i,j}^{n+1})_{rr}^{k+2} + \frac{1}{r_i}(f_{i,j}^{n+1})_r^{k+2} = \rho_k f_{i,j}^{n+1,k+1} + (f_{i,j}^{n+1})_{zz}^{k+1} + r_i g_{i,j}, \quad (31b)$$

where the superscripts n and k indicate, respectively, the time step and the iteration level from which the value of the function f is taken. Equations (31a) and (31b) can be generalized as

$$(\rho_k I + H)\bar{f} = D, \quad (32)$$

where H is a tridiagonal matrix operator, I is the identity matrix, D is a known column vector, and $\bar{f}$ is the solution vector.

The quantities ρ_k in Eq. (31) are iteration parameters which are added to the equation to increase the speed with which convergence to the solution is obtained. The "best" values of the ρ_k are given by Varga (1963) and Young (1962) for a square equally spaced grid for Laplace's equation to be

$$\rho_k = b\left(\frac{a}{b}\right)^{k+1/m+1}, \qquad k = 1, 2, \ldots, m, \quad (33)$$

where a and b are, respectively, the maximum and minimum eigenvalues of the matrix operator H in Eq. (32). Unfortunately, no analytical values of ρ_k can be obtained for the grid and difference equation which we have specified, but Briley's (1968) and our experiments indicate that the values of a and b above and a value of $m = 5$ yield the greatest convergence rate if the values of $f_{i,j}^n$ are used as initial approximations to the values of $f_{i,j}^{n+1}$. We now introduce the finite-difference operators from Eq. (28) into Eq. (12) to obtain

$$\begin{aligned}&\left[\frac{1}{\Delta t_n} + \frac{1}{r_i^2}(f_{i,j}^{n+1})_z + \frac{1}{r_i^2 R}\right] g_{i,j}^{n+1} \\ &\quad - \left[\frac{1}{r_i}(f_{i,j}^{n+1})_z + \frac{1}{r_i R}\right](g_{i,j}^{n+1})_r - \frac{1}{R}(g_{i,j}^{n+1})_{rr} \\ &\quad = \frac{1}{\Delta t_n} g_{i,j}^n - \left[\frac{1}{r_i}(f_{i,j}^n)_r + 1 - r_i^2\right](g_{i,j}^n)_z + \frac{1}{R}(g_{i,j}^n)_{zz} \end{aligned} \quad (34a)$$

and

$$\begin{aligned}&\frac{1}{\Delta t_{n+1}} g_{i,j}^{n+2} + \left[\frac{1}{r_i}(f_{i,j}^{n+2})_r + 1 - r_i^2\right](g_{i,j}^{n+2})_z - \frac{1}{R}(g_{i,j}^{n+2})_{zz} \\ &\quad = \left[\frac{1}{\Delta t_{n+1}} - \frac{1}{r_i^2}(f_{i,j}^{n+1})_z - \frac{1}{r_i^2 R}\right] g_{i,j}^{n+1} \\ &\quad + \left[\frac{1}{r_i}(f_{i,j}^{n+1})_z + \frac{1}{r_i R}\right](g_{i,j}^{n+1})_r + \frac{1}{R}(g_{i,j}^{n+1})_{rr}. \end{aligned} \quad (34b)$$

The time step, Δt_n, must be much less than one, and it must be the same between the $n + 1$ and the $n + 2$ time steps. We have treated the time step as a parameter which may be selected subject to the restriction $\Delta t_{2n+2} = \Delta t_{2n+1}$, in order to improve the convergence of the iterative procedure which must be used to solve the difference equations (31a, b) and (34a, b). The initial value of the time step was 0.02. It was allowed to vary over the range 0.0075–0.025 in order to maintain a stable solution.

We now need to transform the boundary conditions to a finite-difference representation. On the line $r = 0$ ($i = 1$), we have from Eqs. (27a) and (27b)

$$f^n_{1,j} = 0 \tag{35a}$$

and

$$g^n_{1,j} = 0, \tag{35b}$$

respectively, for all j and n. On the line $r = 1$ ($i = I_{\max}$), we have from Eqs. (14), (15), and (26) the conditions that

$$f^n_{I_{\max},j} = 0, \tag{36a}$$

$$\frac{1}{r_{I_{\max}}} \frac{\partial f(r_{I_{\max}})}{\partial r} = 0, \tag{36b}$$

and

$$g^n_{I_{\max},j} = -\frac{1}{r_{I_{\max}}} \frac{\partial^2 f(r_{I_{\max}})}{\partial r^2}, \tag{36c}$$

where the differential operators are described by differentiated Lagrangian interpolation formulas. The difference representations for the boundary conditions specified in Eq. (36) were applied over the range ($I_{\max} - 4 \leqslant i \leqslant I_{\max} + 1$). This range of grid points was used since it was found to yield more accurate results when Eq. (36b) was used to eliminate the stream function value at $I_{\max} + 1$.

From Eqs. (18) and (19) we have for the line $z = 0$ ($j = 1$),

$$\frac{\partial f(z = 0)}{\partial z} = 0 \tag{37a}$$

and

$$g^n_{i,1} = 0. \tag{37b}$$

At the disturbance point $(R_1, Z_1) = (0.6, 2.0)$, we have from Eqs. (22) and (23)

$$f^n_{R_1,Z_1} = \left(\frac{r^2_{R_1}}{2} - \frac{r^4_{R_1}}{4}\right)(A_m \sin A_r t_n) \tag{38a}$$

and

$$g^n_{R_1,Z_1} = -\frac{1}{r_{R_1}}\left[(f^n_{i,j})_{rr} - \frac{1}{r_{R_1}}(f^n_{i,j})_r + (f^n_{i,j})_{zz}\right]. \tag{38b}$$

On the downstream boundary $z = L$ $(j = J_{\max})$, we have from (20) and (21a, b) that

$$\frac{\partial^2 f}{\partial z^2} = 0, \tag{39a}$$

and either

$$\frac{\partial^2 g}{\partial z^2} = 0 \tag{39b}$$

or

$$\frac{\partial g}{\partial z} = 0. \tag{39c}$$

In Eq. (39) the j index has the range $(J_{\max} - 4 \leqslant j \leqslant J_{\max})$. This range of j values is used to avoid using function values at points located outside the flow field. The boundary conditions which we used are Eqs. (39a) and (39c).

The initial conditions are given from Eqs. (22) and (23) as

$$f^0_{i,j} = 0 \tag{40a}$$

and

$$g^0_{i,j} = 0. \tag{40b}$$

The difference equations (31a, b) and (34a, b) are written to be solved using an adaptation of the ADI method subject to the boundary conditions, Eqs. (35)–(40). The ADI method employed is an adaptation of a technique of Varga (1963).

In a nonlinear set of coupled partial differential equations such as (12) and (13) no linearization can give a totally correct solution, as witnessed by the failure of linearized stability theory to predict transition for Poiseuille pipe flow. In order to determine analytically what the correct approximations are to Eqs. (12) and (13), it would be necessary to either linearize them or their nonlinear approximations and study the form of the resulting approximation, truncation, and round-off errors. A similar approach has been taken by Fromm and Harlow (1963) and Fromm (1963) for a rectangular coordinate system. However, it was felt

that an experimental verification of correctness should be sufficient since our systems of approximations (31) and (34) are consistent with Eqs. (12) aud (13) under our solution sequence. Several different mesh combinations were considered in attempting to obtain the optimum mesh spacing. We found that uniform spacings of 0.1 and 0.05 in both coordinate directions yielded essentially the same results; therefore, we chose a spacing of 0.1. This, consistent with the time step mentioned earlier, generated a stable solution.

Before explaining the calculation procedure, we set forward the convergence tests that are applied. For the stream function we used

$$| f_{i,j}^{n,l,k+2m} - f_{i,j}^{n,l,k} | \leqslant \epsilon_f [\max_{i,j} | f_{i,j}^{n,l,k+2m-1} |], \tag{41}$$

where m is the number of ρ values used in the iterative procedure and k is the stream-function iteration counter. We chose ϵ_f such that $\epsilon_f \leqslant 1.0 \times 10^{-5}$.

The tests used for convergence of the vorticity are

$$| g_{i,j}^{m,l,k+2+1} - g_{i,j}^{n,l} | \leqslant \epsilon_{g_i} [\max_{i,j} | g_{i,j}^{n,l} |] \; i \neq I_{\max}, \tag{42a}$$

and

$$| g_{I_{\max},j}^{n,l+1} - g_{I_{\max},j}^{n,l} | \leqslant \epsilon_{g_b} [\max_{j} | g_{I_{\max},j}^{n,l} |]. \tag{42b}$$

In Eqs. (41) and (42) l is the vorticity iteration counter. Equation (42a) was used where $i < I_{\max}$ and Eq. (42b) was used when $i = I_{\max}$. We demanded that $\epsilon_{g_b} = 2\epsilon_{g_i}$, and that $\epsilon_{g_b} \geqslant \epsilon_f$ at all iterations. We recognize that these convergence tests are intuitive rather than mathematical, for we know of no theoretical criterion for convergence. Our convergence criteria come under the classification of Birkhoff's (1960) "plausible intuitive hypothesis."

The vorticity and stream function calculations are stopped when

$$T > 20, \tag{43}$$

where T is the real time, or when a solution pattern was established.

The solution to the difference equations is accomplished iteratively by first advancing the vorticity using Eqs. (34a, b) for alternate time steps. Then Eqs. (31a, b) are iterated to convergence and the vorticity is recalculated on the basis of the updated stream function. This sequence is continued until the vorticity converges. Then the process is begun again in sequence with the alternate equation of Eqs. (34a, b) for the next time step.

4. Results and Discussion

Five examples have been chosen to provide the means of determining the stability of Poiseuille pipe flow. The examples will be referred to as Cases 1–5 and are as follows: Case 1 is for a Reynolds number of 1000 and a disturbance amplitude, A_m from Eq. (38a), equal to 1.0. Reynolds numbers of 3000, 10,000 and 100,000, each at an amplitude of 1.0, represent Cases 2, 3, and 4, respectively. Case 5 is at a Reynolds number of 100,000 and an amplitude of 0.1.

The results for all cases were calculated with the disturbance located at the point $(R_1, Z_1) = (0.6, 2.0)$ on a square mesh of size 0.10 and with an initial time step of 0.02. The criterion for stability was taken to be the decrease in maximum value of the disturbance stream function with axial distance. The time necessary to compute the solutions for Cases 1–5 varied from 5 to $6\frac{1}{2}$ hours of Scientific Data Systems SIGMA 7 computer time. These computation times are quite reasonable when one realizes that all computations were performed in double precision and that a stream function was computed for each iteration of the vorticity. The calculation of more stream functions than might be thought necessary (see Dixon and Hellums (1967)) is mandatory for the consistency of the difference and differential equations. It might also be noted that double-precision operation in SIGMA 7 is a factor of 8–16 times slower than a CDC 6600. For a more complete discussion of the results obtained or for plots of the stream function and vorticity versus axial distance, see Crowder and Dalton (1969).

The first four cases are finite-amplitude disturbances since we have taken these stream function disturbances to be on the same order of magnitude as the fully developed flow stream function at the location of the disturbance. The remaining case, Case 5, represents a small-amplitude disturbance since the A_m value has been taken to be an order of magnitude less than the fully developed flow stream function of the location of the disturbance.

The criterion used for determining when a flow example was stable was based on whether or not the disturbance stream function was amplified as downstream motion occurred. If the disturbance decays with increasing axial distance, then the flow is deemed stable; if not, then the flow is considered unstable.

In considering the detailed calculations for each example, it was noted that the maximum value of the disturbance stream function and vorticity moved off the radial line on which the disturbance was applied as downstream motion progressed. It was felt that, to represent the solutions accurately, the maximum disturbance values needed to be located for each solution time step since these maximum values truly represented the disturbance behavior. Therefore, the results are given in terms of the maximum disturbance values as the disturbance wave moves downstream.

Case 1, for a Reynolds number of 1000 and a disturbance amplitude of 1.0,

is depicted in Fig. 1. The behavior of the maxima of the disturbance stream function is shown in Fig. 1a, which shows that the disturbance grows to a value of 0.22 and then decreases to a value of about 0.15 at an axial distance of 3.5 and a time of 2.006. For greater times, as the disturbance continues to move downstream, the stream function values continue to decrease although on a more gradual scale. In essence, Fig. 1a is showing that Case 1 is satisfying the stability

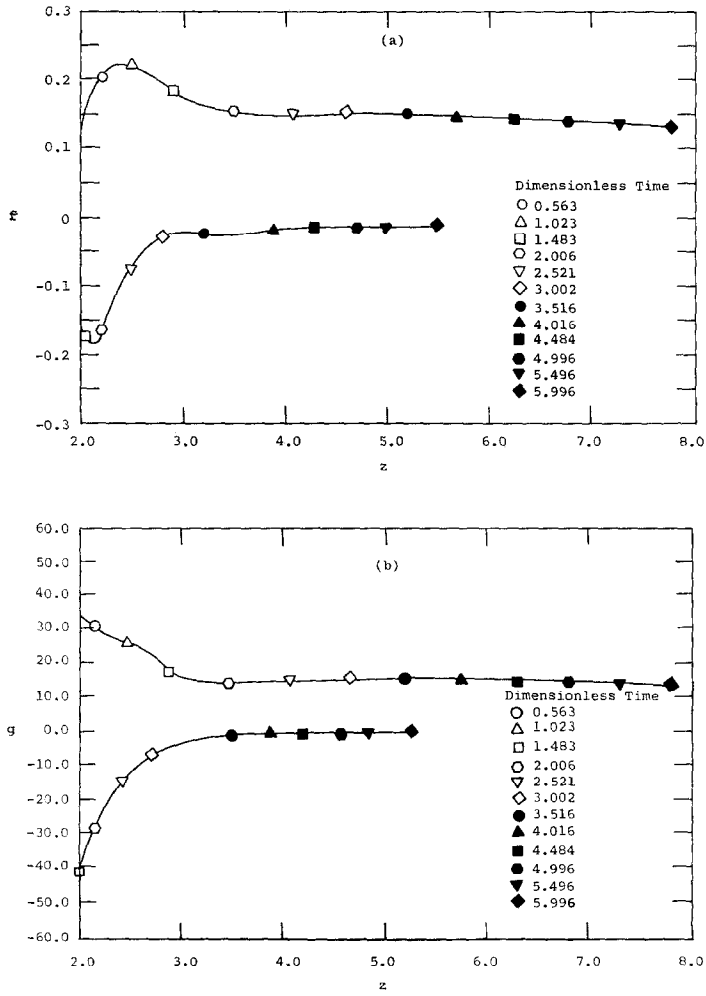

FIG. 1. (a) Maximum value of disturbance stream function vs downstream distance, $R = 10^3$, $A_m = 1.0$, $A_r = \pi$. (b) Maximum value of disturbance vorticity vs downstream distance, $R = 10^8$, $A_m = 1.0$, $A_r = \pi$.

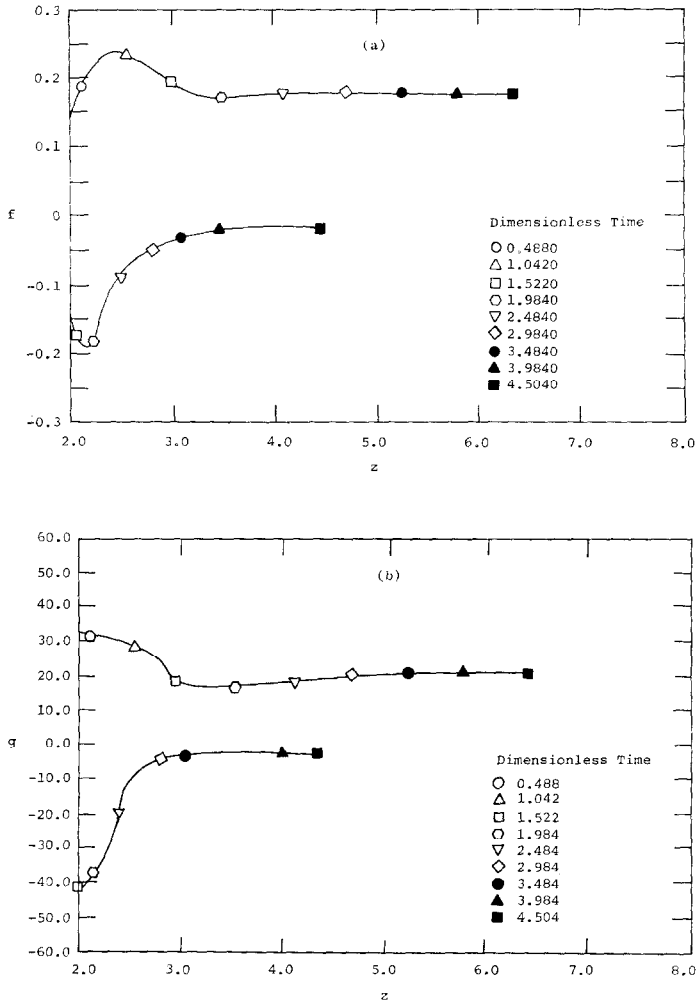

FIG. 2. (a) Maximum value of disturbance stream function vs downstream distance, $R = 3 \times 10^3$, $A_m = 1.0$, $A_r = \pi$. (b) Maximum value of disturbance vorticity vs downstream distance, $R = 3 \times 10^3$, $A_m = 1.0$, $A_r = \pi$.

criterion imposed earlier in this section. At a Reynolds number of 1000, it has been found that Poiseuille pipe flow is stable when subjected to a finite-amplitude disturbance, Leite (1959). The results presented here indicate that the experimental observation is verified. The disturbance vorticity plot, Fig. 1b, corroborates this conclusion.

At a Reynolds number of 3000 and an amplitude of 1.0, Case 2, the calculations plotted in Fig. 2 show that the disturbance quantities are not decaying with downstream distance; however, neither are they amplifying. Hence, Case 2 is deemed to be a neutrally stable situation. Experiments at this Reynolds number have been inconclusive in setting a rigid physical criterion for instability.

At an amplitude of 1.0 and a Reynolds number of 10,000, Case 3, it is seen

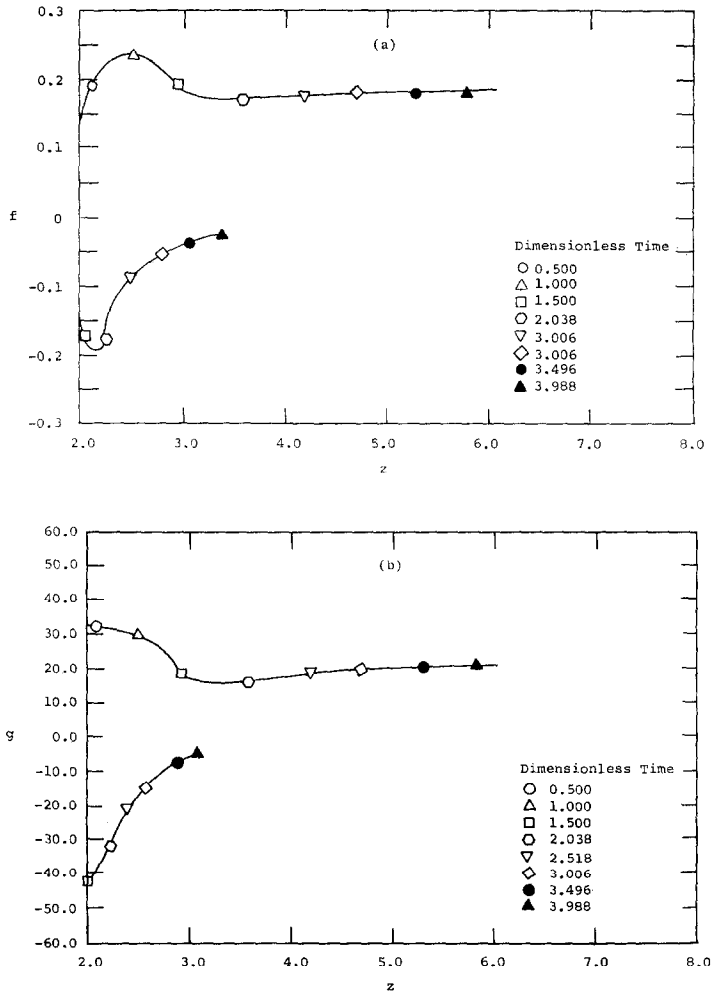

FIG. 3. (a) Maximum value of disturbance stream function vs downstream distance, $R = 10^4$, $A_m = 1.0$, $A_r = \pi$. (b) Maximum value of disturbance vorticity vs downstream distance, $R = 10^4$, $A_m = 1.0$, $A_r = \pi$.

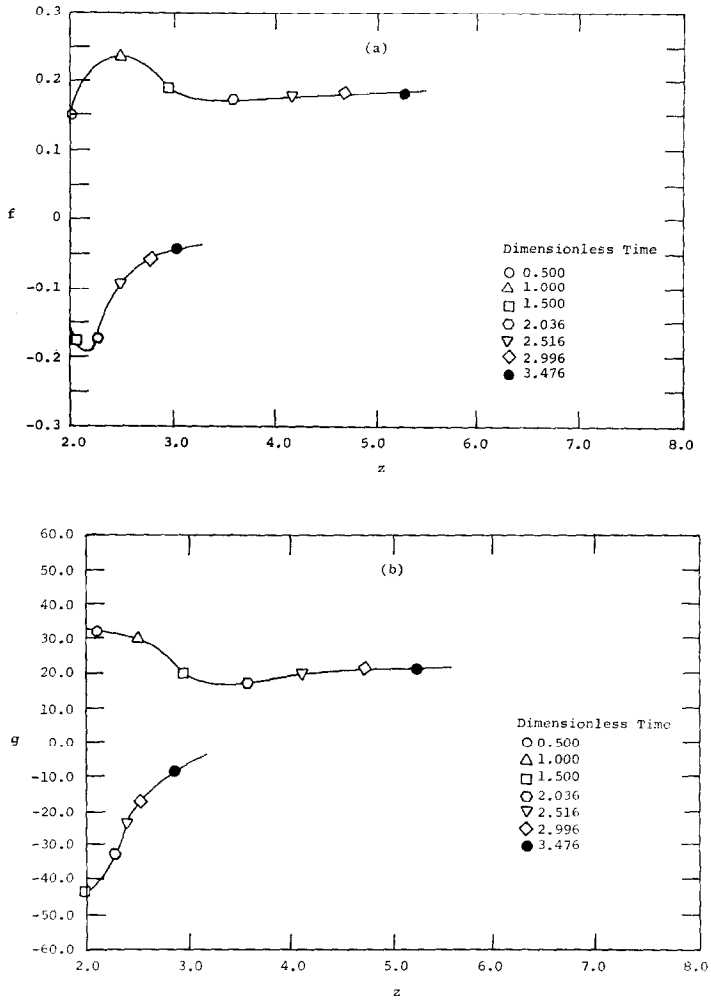

FIG. 4. (a) Maximum value of disturbance stream function vs downstream distance, $R = 10^5$, $A_m = 1.0$, $A_\tau = \pi$. (b) Maximum value of disturbance vorticity vs downstream distance, $R = 10^5$, $A_m = 1.0$, $A_\tau = \pi$.

that the disturbance quantities are slightly increasing with downstream distance. This implies instability according to the criterion established earlier. Physically, instability is expected at a Reynolds number this large for a sufficiently large disturbance. Therefore, the failure of the calculated values to decay infers instability. Furthermore, the calculation procedure failed to converge past a computation time of 3.988 in spite of several corrective attempts (which included considering

smaller time steps). The failure to converge is taken as further evidence of instability.

The largest Reynolds number case, Case 4, at an amplitude of 1.0, is expected to be highly unstable in a physical situation. The results for this calculation, shown in Figs. 4a and 4b, are similar to those noted for Case 3. The increasing maximum amplitude of the disturbance stream function with downstream progres-

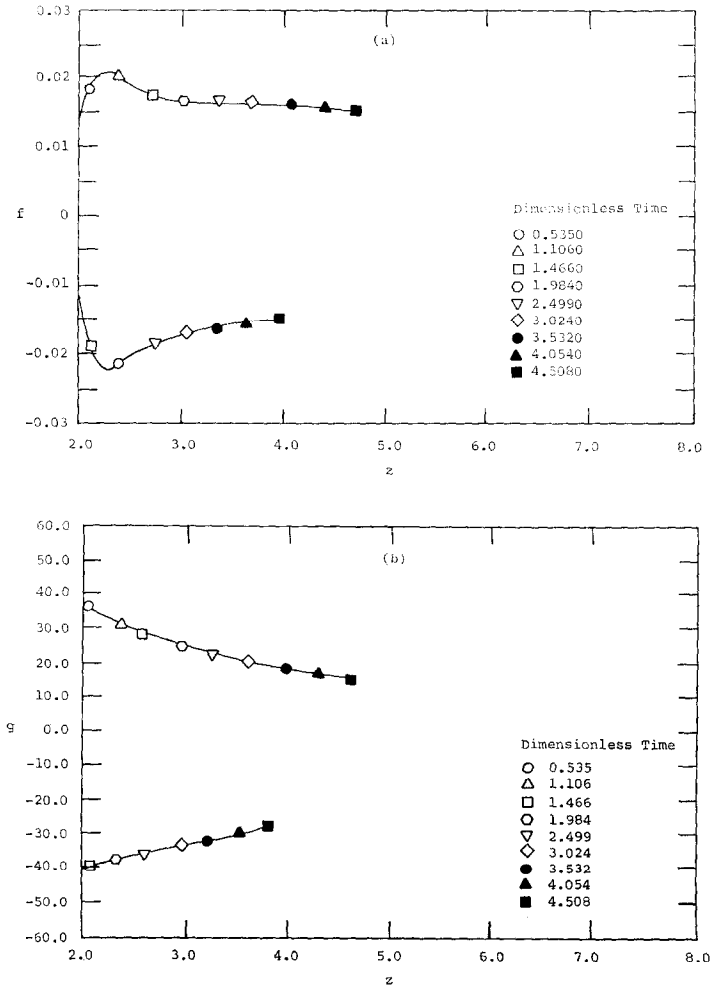

FIG. 5. (a) Maximum value of disturbance stream function vs downstream distance, $R = 10^5$, $A_m = 0.1$, $A_r = \pi$. (b) Maximum value of disturbance vorticity vs downstream distance, $R = 10^6$, $A_m = 0.1$, $A_r = \pi$.

sion is taken to represent instability. This conclusion is further corroborated by the failure of the solution to converge, as happened in Case 3. Both features taken together strongly suggest instability. Because of the higher Reynolds number, the results obtained for Case 4 are considered to strengthen the observations made for Case 3.

The small-amplitude case, Case 5, is taken at a Reynolds number of 100,000 and an amplitude of 0.1. If the numerical solution is to be consistent with classical instability theory, then Case 5 should yield a stable solution. This is, in fact, the actual case. Figure 5 shows a fairly steady and relatively strong decrease in both of the disturbance functions. These results (and their consistently smaller magnitudes when compared to the other cases) suggest stability.

5. Summary and Conclusions

The feasibility of a numerical technique to determine the response of Poiseuille pipe flow to a given disturbance has been demonstrated. This problem has been treated experimentally many times with well-substantiated results which serve as a basis for comparison with the present approach.

The results of the preceding section demonstrate that the numerical approach contained herein does yield a stable solution to an axisymmetric disturbance of the form $f(R_1, Z_1, t_n) = (1.0) \cdot ((R_1^2/2) - (R_1^4/4)) \sin \pi t_n$ at a Reynolds number of 1000. The stream function disturbance is seen to decay with downstream axial distance for this example.

At a Reynolds number of 3000 and a disturbance amplitude of 1.0, the disturbance stream function is not seen to decay with increasing downstream distance; however, no growth of the disturbance stream function is noted either. This Reynolds number calculation seems to be neutrally stable.

For a Reynolds number of 10,000, the same disturbance function was found not to decay but was carried downstream with slightly increasing amplitude. This result failed to meet our stability criterion cited in Section 4, i.e., if the amplitude of the maximum value of the disturbance stream function decays with downstream axial distance, then the flow is deemed stable to the disturbance at the given Reynolds number.

At a Reynolds number of 100,000 and a disturbance amplitude of 1.0, the stream function disturbance was also amplified with downstream axial distance. This is definitely an unstable condition according to the cited criterion.

The four examples for which results have been cited were all for a disturbance amplitude of 1.0 which is, of course, a finite-amplitude disturbance. The results of these calculations have been consistent with what is expected from the physical

problem for the same conditions. To examine what would happen for a small-amplitude disturbance, we considered a flow with Reynolds number of 100,000 and a disturbance amplitude of 0.1. We found for this case that the disturbance was definitely damped as it progressed downstream.

On the basis of preliminary, short computer runs, it was found that, to insure numerical stability and improve accuracy of the solution, an equally spaced grid was necessary for the solution of the finite-difference equations.

For the disturbance used, a flow field of 14 radii appears to be of sufficient length to represent an "infinite" length for the times covered by these calculations. Double-precision arithmetic was found to improve the numerical stability of the solution and to speed the convergence as well as reducing total computing time.

In conclusion, we say that Poiseuille pipe flow is unstable to an axisymmetric disturbance of the form $f(R_1, Z_1, t_n) = (1.0) \cdot ((R_1^2/2) - (R_1^2/4)) \sin \pi t_n$ at Reynolds numbers of 10,000 and 100,000 is stable at a Reynolds number of 1000 and is neutrally stable at 3000. When the disturbance amplitude is changed from 1.0 to 0.1 at a Reynolds number of 100,000, we found that the flow was stable.

Acknowledgments

One of the authors (HJC) was on educational leave of absence from Bellaire Research Laboratories, Texaco, Inc., and was a NASA Trainee during the investigation.

References

Bhat, W. V., 1966, Ph.D. Dissertation, University of Rochester, New York.
Birkhoff, G., 1960, "Hydrodynamics," Princeton U. Press, Princeton, N. J.
Briley, W. R., 1968, Ph.D. Dissertation, University of Texas at Austin, Texas.
Corcos, G. M., and Sellars, J. R., 1959, *J. Fluid Mech.* **5**, 97.
Crowder, H. J., and Dalton, C., 1969, Final Report on NASA Contract NGR No. 44-005-065.
Davey, A., and Drazin, P. G., 1969, *J. Fluid Mech.* **36**, 209.
Dennis, S. C. R., and Shimshoni, M., 1964, Aero. Res. Coun. CP 797, London, England.
Dixon, T. N., and Hellums, J. D., 1967, *AIChE J.* **13**, 866.
Fromm, J. E., and Harlow, F. H., 1963, *Phys. Fluids* **6**, 975.
Fromm, J. E., 1963, Los Alamos Scientific Laboratory Report No. 2910.
Gill, A. E., 1965, *J. Fluid Mech.* **21**, 145.
Graebel, W., 1970, *J. Fluid. Mech.*, **43**, 279.
Greenspan, D., *et al.*, 1964, MRC-TS Rpt. 482, University of Wisconsin, Madison, Wisconsin.
Harlow, F. H., and Fromm, J. E., 1964, *Phys. Fluids* **7**, 1147.
Hirota, I., and Miyakoda, K., 1965, *J. Met. Soc. Japan* **43**, 30.
Ingham, D. B., 1968, *J. Fluid Mech.* **31**, 815.
Kuethe, A. M., 1956, *J. Aero. Sci.* **23**, 444.
Leite, R. J., 1959, *J. Fluid Mech.* **5**, 81.

PAYNE, R. B., 1958, *J. Fluid Mech.* **4**, 81.
PEKERIS, C. L., 1948, *Proc. Nat. Acad. Sci. U.S.A.* **34**, 285.
REYNOLDS, O., 1880, *Phil. Trans. Roy. Soc.* **174**, 935.
SEXL, T., 1927, *Ann. Phys. (New York)* **83**, 835.
STUART, J. T., 1958, *J. Fluid Mech.* **4**, 1.
TATSUMI, T., 1952, *J. Phys. Soc. Japan* **7**, 495.
THOMAN, D. C., AND SZEWCZYK, A. A., 1969, II-76.
VARGA, R. S., 1963, "Matrix Iterative Analysis," Prentice-Hall, Englewood Cliffs, N. J.
YOUNG, D. M., 1962, *in* "Survey of Numerical Analysis" (J. Todd, Ed.), McGraw-Hill, New York.